A Sensorless DTC Strategy of Induction Motor Fed by Three-level Inverter Based on Discrete Space Vector Modulation

Yongchang Zhang, Jianguo Zhu, Youguang Guo, Wei Xu
School of Electrical, Mechanical and Mechatronic Systems
University of Technology, Sydney, NSW 2007
Sydney, Australia
zhangdavid37@gmail.com

Zhengming Zhao
Department of Electrical Engineering
Tsinghua University
Beijing, China
zhaozm@tsinghua.edu.cn

***Abstract*—A sensorless direct torque controlled (DTC) induction motor drive fed by a 3-level inverter is presented based on discrete space vector modulation. A novel vector synthesis sequence is proposed to solve the problems caused by the topology of the 3-level inverter, such as neutral point unbalance and excessive voltage jump, while maintaining the merits of simplicity and robustness. Fuzzy logic control and speed adaptive flux observer are introduced to enhance the performance of system. The problem of large starting current is investigated and solved by introducing the technique of pre-excitation. A 32-bit fixed-point DSP based 3-level motor drive has been developed and a series of experimental results are presented to confirm the effectiveness of the proposed techniques.**

Keywords-sensorless; direct torque control (DTC); induction motor; 3-level inverter; discrete space vector modulation; fuzzy logic.

I. INTRODUCTION

Direct torque control (DTC) is characterized by its merits of fast torque response, simple structure and strong robustness against stator parameter variations, and has been extensively studied and investigated since it was firstly proposed by Takahashi [1] and Depenbrock [2]. For high voltage high power application, the 3-level inverter-fed motor drive is an appropriate approach, as it provides better performance than the conventional 2-level inverter in terms of lower voltage stress across the semiconductor switches, less harmonic content and lower switching frequency [3]. Because the 3-level DTC induction motor (IM) drive combines the merits of both 3-level inverter and DTC, it has attracted more and more attention, especially in high power drive applications.

There are usually ripples in flux and toruqe for conventional 2-level DTC, especially in the low speed range, which deteriorates the system performance. This is caused by that the switching table for classical DTC is composed of limited number of discrete vectors, and the selected vector will work in the whole duration of one sampling period. Also, the selection of vector depends only on the signs of torque and flux errors without considering their magnitudes; this sometimes makes the selection of vector inaccurate. A lot of papers [4]-[5] have been published on overcoming this problem, and most of them adopted continuous space vector modulation (SVM) to produce continuous reference space voltage vector, which can be generated by using the proportional integral controller (PI), sliding mode controller (SMC), dead-beat controller or predictive controller, etc. Continuous SVM smoothes the response of flux and torque, but increases the complexity of system and decreases the robustness of DTC. To preserve the simplicity and robustness of DTC and decrease the ripples in flux and torque, a modified DTC with discrete space vector modulation (DSVM) was proposed in [6] by Casadei, which incorporates a more complicated and accurate switch table by dividing one sampling period into 2 or 3 intervals, and thus more vectors are obtained. Also, speed is taken into account and more levels of hysteresis are adopted to make the switching table more accurate. However, [6] was aiming at the 2-level DTC, so the 3-level DTC was not addressed.

To make the 3-level DTC motor drive applicable, there are some problems which should be resolved. Firstly, the potential of neutral point should be well controlled to avoid higher voltage stress across semiconductors, which means increased capacity and cost. Secondly, the switching between any two vectors should be smooth to decrease harmonic content and switching loss. Thirdly, low speed operation with excellent performance should be guaranteed to obtain wide speed range, especially for speed sensorless operation. Finally, the starting current should be controlled effectively to guarantee safe operation of 3-level inverter and decrease the current capacity requirement of semiconductors. As there is no inner current loop in DTC, this problem should be handled carefully.

This paper employs the DSVM in the 3-level DTC, and a novel vector synthesis sequence is proposed to solve the above –mentioned problems, including the neutral point unbalance and excessive vector switching. To improve the low speed performance, especially under sensorless condition, a speed adaptive flux observer with torque observation is introduced and fuzzy logic controller (FLC) is used in the outer speed loop to enhance the speed response. The problem of large starting current is addressed and solved by introducing the technique of pre-excitation. A series of experimental results are presented to validate the effectiveness of the schemes proposed in this paper.

II. VECTOR SYNTHESIS SEQUENCE FOR DSVM

A. Principle of DTC

The mathematical model of an induction motor described by space vectors in a stationary frame can be expressed as

$$\boldsymbol{u}_s = R_s \boldsymbol{i}_s + p\boldsymbol{\psi}_s \tag{1}$$

$$0 = R_r \boldsymbol{i}_r + p\boldsymbol{\psi}_r - j\omega_r \boldsymbol{\psi}_s \tag{2}$$

$$\boldsymbol{\psi}_s = L_s \boldsymbol{i}_r + L_m \boldsymbol{i}_r \tag{3}$$

$$\boldsymbol{\psi}_r = L_m \boldsymbol{i}_s + L_r \boldsymbol{i}_r \tag{4}$$

where $\boldsymbol{u_s}$, $\boldsymbol{i_s}$, $\boldsymbol{i_r}$, $\boldsymbol{\psi_s}$ and $\boldsymbol{\psi_r}$ are the stator voltage vector, stator current vector, rotor current vector, stator flux linkage vector and rotor flux linkage vector, respectively; R_s, R_r, L_s, L_r, L_m and N_p are the stator resistance, rotor resistance, stator inductance, rotor inductance, mutual inductance and motor pole-pair number; and ω_r is the rotor speed.

From the stator voltage equation (1), it can be seen that, by omitting the stator resistance voltage drop, the stator flux can be controlled directly by the stator voltage. This is a crude analysis and may cause error at low speed.

The electromagnetic torque is expressed as (5)

$$T_e = \frac{3}{2} N_p \frac{L_m}{\sigma L_s L_r} \boldsymbol{\psi}_r \otimes \boldsymbol{\psi}_s = \frac{3}{2} N_p \frac{L_m}{\sigma L_s L_r} \|\boldsymbol{\psi}_r\| \|\boldsymbol{\psi}_s\| \sin \delta_{sr} \tag{5}$$

where δ_{sr} is the spatial angle between stator flux and rotor flux and T_e is the electromagnetic torque. In DTC, the amplitude of the stator flux is kept constant and a fast torque response is obtained by changing angle δ_{sr} quickly. From (1)-(4), the relationship between the stator flux and the rotor flux can be obtained from

$$p\boldsymbol{\psi}_r + \left(\frac{1}{\sigma T_r} - j\omega_r\right)\boldsymbol{\psi}_r = \frac{L_m}{\sigma L_s T_r} \boldsymbol{\psi}_s \tag{6}$$

where $\sigma = 1 - L_m^2 / (L_s L_r)$ and $T_r = L_r / R_r$. Eqn. (6) indicates that the dynamic response of the rotor flux is first-order lagged with respect to the stator flux. In fast dynamic response, rotor flux can be considered as constant compared to stator flux during one sampling period, and the amplitude of stator flux is kept constant by using the closed-loop control. Hence, fast torque response can be obtained by changing the angle of stator flux.

B. Novel DSVM for 3-level DTC

DSVM was firstly applied in 2-level DTC [6] and its main aim is to reduce the ripples in torque and flux. For 3-level DTC, not only the ripples in torque and flux at low speed operation should be reduced, but also the problems of neutral point unbalance and non-smooth switching between any two arbitrary vectors should be considered, which are of vital importance for the practicability of 3-level DTC.

Smooth vector switching means that there is no big jump in phase voltage or line voltage. High voltage jump increases the harmonic content and stress across power semiconductors, which negate the advantages of the 3-level inverter. Furthermore, 3-phase jump at the same time is not allowed as it would increase the switching frequency and loss.

Neutral point balance is very important for a 3-level inverter, because any unbalance will cause higher voltage in the power semiconductors, which increases the demand of capacity so that the cost increases. Many papers have investigated on this problem and various methods have been proposed. These methods can be divided into three groups [7]: passive control, active control and hysteresis control. Hysteresis control is simple and robust, so it is employed in this paper. When the neutral point potential exceeds the hysteresis range, the neutral point control will work by adjusting the duty ratio of the small vectors in a vector sequence according to the directions of three phase load currents and the drift direction of the neutral point potential.

By using the DSVM, we can firstly construct some synthesis vectors which can solve the problems of neutral point unbalance and non-smooth switching between any two vectors simultaneously. The synthesis vectors are selected according to the demand of flux and torque. There are 27 voltage space vectors as illustrated in Fig. 1. However, the 27 vectors are not directly used. A series of novel synthesis vectors are used instead, which are illustrated in Fig. 2 and marked by $\mathbf{V}_{s1}$, $\mathbf{V}_{s2}$,…, $\mathbf{V}_{s12}$. The angle of each synthesis vector is fixed and its amplitude can be variable or constant. In this paper, constant amplitude of synthesis vector is selected for simplicity. The novel vector synthesis sequence is listed in Table I and the sector division for 3-level DTC is presented in Table II. From Table I it is seen that the switching between any arbitrary two vectors or adjacent vectors in a synthesis sequence is smooth. The neutral point unbalance can be solved by adjusting the lasting time of small vectors in one sapling period. Taking $\mathbf{V}_{s1}$ as an example, 211 and 100 are a pair of small vectors and their total lasting time is fixed, but their individual working time can be arranged according to the demand of neutral point balance.

Table II shows the principle of vector selection for 3-level DTC. To obtain good performance and not increase the complexity dramatically, three-level hysteresis control is used for both flux and torque, where *k* stands for the number of sector where the stator flux locates and it is cycling counted, which means that when the selected vector number exceeds the range, it will be added or subtracted by 12.

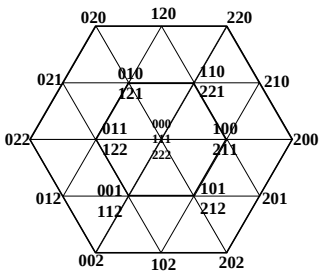

Figure 1. 3-level inverter vector diagram

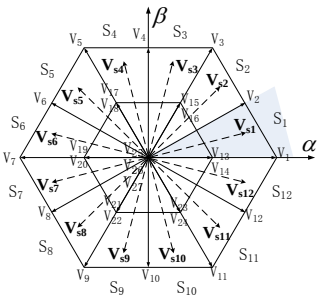

Figure 2. Synthesis vector diagram

TABLE I. NOVEL VECTOR SYNTHESIS

Vector no.	Vector synthesis sequence
$\mathbf{V}_{s1}$	111-211-210-200-100-200-210-211-111
$\mathbf{V}_{s2}$	111-110-210-220-221-220-210-110-111
$\mathbf{V}_{s3}$	111-110-120-220-221-220-120-110-111
$\mathbf{V}_{s4}$	111-121-120-020-010-020-120-121-111
$\mathbf{V}_{s5}$	111-121-021-020-010-020-021-121-111
$\mathbf{V}_{s6}$	111-011-021-022-122-022-021-011-111
$\mathbf{V}_{s7}$	111-011-012-022-122-022-012-011-111
$\mathbf{V}_{s8}$	111-112-012-002-001-002-012-112-111
$\mathbf{V}_{s9}$	111-112-102-002-001-002-102-112-111
$\mathbf{V}_{s10}$	111-101-102-202-212-202-102-101-111
$\mathbf{V}_{s11}$	111-101-201-202-212-202-201-101-111
$\mathbf{V}_{s12}$	111-211-201-200-100-200-201-211-111

TABLE II. VECTOR SELECTION FOR 3-LEVEL DTC

Flux	Torque	Selected vector number
↑	↑	k + 2
	=	26
	↓	k - 2
↓	↑	k + 4
	=	26
	↓	k - 4
=	↑	k + 3
	=	26
	↓	k-3

C. *Decreasing Starting Current*

As mentioned in Section I, there usually exists a large starting current in the DTC motor drive, which increases the demand for the capacity of power electronics switches and may cause neutral point unbalance, so it is necessary to restrict the starting current. This paper employs the pre-excitation technique to reduce starting current while maintaining enough starting torque. The stator flux is firstly established by applying a certain large voltage vector, e.g. 200. During the pre-excitation process, the starting current is sampled and when it reaches the setting maximum current, the zero vector will be selected to decrease the current, which acts in a bang-bang fashion. When the stator flux reaches the commanding value, the pre-excitation process is finished and the motor can start up with a sufficient torque.

III. FLC AND SPEED ADAPTIVE FLUX OBSERVER

To enhance the dynamic performance and steady accuracy, as well as robustness to external disturbance and motor parameters variations, fuzzy logic controller (FLC) is used in the outer speed loop. The FLC can handle complicated nonlinear systems with uncertainty, and does not require exact system model and parameters; this makes the FLC very suitable for motor drives [8].

Motor drive without sensors can work under hostile environments, which increase the reliability and decrease the complexity and cost of the system, thus sensorless operation is very attractive for industry application. Among various sensorless approaches, observer-based techniques are very popular and versatile. Compared with open-loop speed estimation techniques, the observer-based methods are more robust against motor parameter variations by introducing the error feedback of stator current estimation. A full-order speed adaptive flux observer with novel gains is employed in this paper, and a load torque observation is introduced to improve the dynamic response of speed estimation [9].

This paper aims to combine the merits of both FLC and speed adaptive full-order observer to improve the performance of low speed operation. The principles are presented in detail.

A. *Fuzzy Logic Speed Control*

FLC is based on the fuzzy set theory which incorporates human experience in the controller. A classical FLC is composed of three parts: fuzzification of input variables, fuzzy reasoning and defuzzification. The diagram of FLC used in this paper is illustrated in Fig. 3. The inputs are the error between commanding value and real value and its derivative, and the output is the control increment *du*, whose integral is the real output. The input and output variables are scaled to the range of (-1.4, 1.4) and there are 9 variables defined in the fuzzy sets: PVB, PB, PM, PS, Z, NS, NM, NB, NVB, in descending order. Figs. 4 and 5 show the membership functions of the input and the output, respectively. To obtain fast response for dynamic performance and high accuracy for steady state, asymmetric triangle is selected as the membership function, which is different from the conventional design. Table III shows the inference rule used in this paper, which is the key part of FLC. By well designing the inference rule, excellent performance can be achieved. The mapping relationship between input variables and output variable is illustrated in Fig. 6.

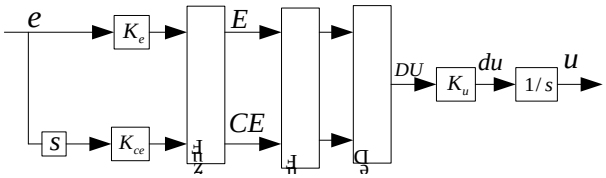

Figure 3. Diagram of FLC

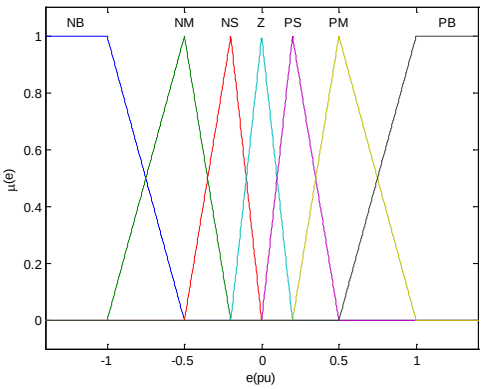

Figure 4. Input membership function

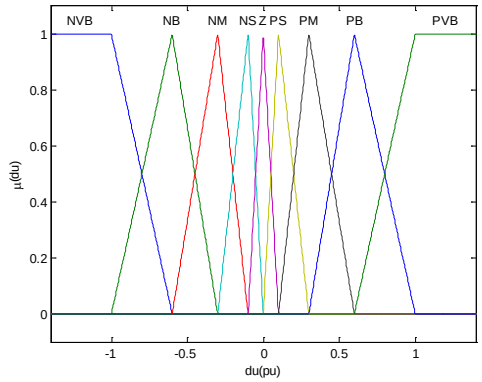

Figure 5. Output membership function

TABLE III. RULE MATRIX OF FLC

Output		Input 1(E)						
		NB	NM	NS	Z	PS	PM	PB
Input 2(CE)	NB	NVB	NVB	NVB	NB	NM	NS	Z
	NM	NVB	NVB	NB	NM	NS	Z	PS
	NS	NVB	NB	NM	NS	Z	PS	PM
	Z	NB	NM	NS	Z	PS	PM	PB
	PS	NM	NS	Z	PS	PM	PB	PVB
	PM	NS	Z	PS	PM	PB	PVB	PVB
	PB	Z	PS	PM	PB	PVB	PVB	PVB

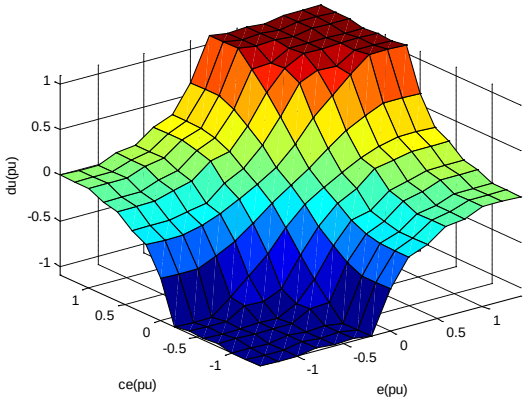

Figure 6. Control surface of FLC

B. *Speed Adaptive Flux Observer*

This paper adopts a novel speed adaptive flux observer with novel gains and a load torque observation, which employs the mechanical equation to improve the dynamic performance. The mathematical model of observer is express as [9]

$$p\hat{\hat{\boldsymbol{i}}}_s = -\left[\left(\frac{1}{\sigma T_s}+\frac{1}{\sigma T_r}\right)-j\omega_r\right]\boldsymbol{i}_s + \frac{1}{\sigma L_s}\left(\frac{1}{T_r}-j\omega_r\right)\hat{\boldsymbol{\psi}}_s + \frac{1}{\sigma L_s}\boldsymbol{u}_s + G_1\left(\boldsymbol{i}_s-\hat{\boldsymbol{i}}_s\right) \tag{7}$$

$$p\hat{\boldsymbol{\psi}}_s = -R_s\hat{\hat{\boldsymbol{i}}}_s + \boldsymbol{u}_s + G_2\left(\boldsymbol{i}_s-\boldsymbol{i}_s\right) \tag{8}$$

$$\frac{d\hat{\omega}_r}{dt} = \frac{N_p}{J}\left(\hat{\hat{T}}_e-T_L\right) + K_\omega\left[\Delta\boldsymbol{i}_s\otimes\left(\lambda L_r\hat{\boldsymbol{\psi}}_s-\hat{\boldsymbol{i}}_s\right)\right] \tag{9}$$

$$\frac{d\hat{T}_L}{dt} = -K_T\left[\Delta\boldsymbol{i}_s\otimes\left(\lambda L_r\hat{\boldsymbol{\psi}}_s-\hat{\boldsymbol{i}}_s\right)\right] \tag{10}$$

where $\hat{\boldsymbol{i}}_s$ and $\hat{\boldsymbol{\psi}}_s$ are the estimated stator current and stator flux, respectively; $G_1=-(g_{1r}+jg_{1i})$ and $G_2=-(g_{2r}+jg_{2i})$ are the observer gains, and K_ω and K_T are the positive constant gains. This paper employs novel observer gains [9] to improve the stability of observer and they are expressed as

$$g_{1r}=2b \tag{11}$$

$$g_{1i}=0 \tag{12}$$

$$g_{2r}=b/(\lambda L_r) \tag{13}$$

$$g_{2i}=0 \tag{14}$$

where b is a negative constant gain.

IV. EXPERIMENTAL RESULTS

To validate the effectiveness of the techniques proposed in this paper, a 3-level DTC motor drive has been developed and experimental results are presented. The whole diagram of the sensorless 3-level DTC drive is illustrated in Fig. 7. FLC is employed in the outer speed loop for speed control, and a speed adaptive flux observer with load torque observation is used to estimate the rotor speed, stator flux and torque and feedback them to the outer loop of speed and flux. The system parameters for the experiment are listed in Table IV. The motor inertia is 0.05 kg·m^2, and the sampling frequency of system is 10 kHz.

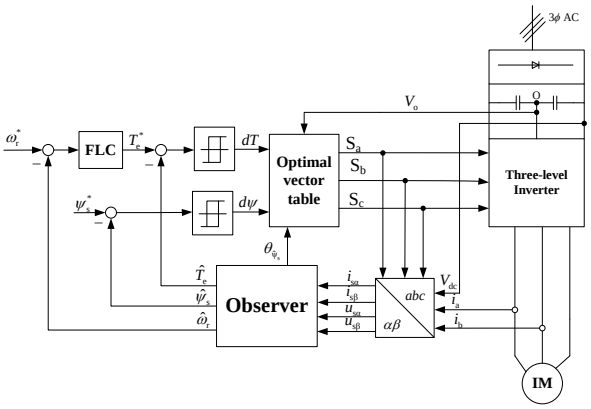

Figure 7. Sensorless 3-level DTC Drive

TABLE IV. SYSTEM AND EXPERIMENTAL PARAMETERS

DC-bus voltage [V]	V_{dc}	560
Rated motor power [kW]	P_N	2.2
Rated motor voltage [V]	U_N	380
Rated (Based) motor frequency [Hz]	f_N	50
Number of motor pairs	N_p	2
Motor stator resistance [Ω]	R_s	2.845
Motor rotor resistance [Ω]	R_r	2.413
Motor mutual inductance [H]	L_m	0.2687
Motor stator inductance [H]	L_s	0.2815
Motor rotor inductance [H]	L_r	0.2815

A. *Experimental Setup*

A three-level inverter-fed induction motor drive has been setup to validate the techniques proposed in this paper. The drive system is composed of four parts: the 3-level inverter, 32-bit fixed-point DSP 2812 based control board and sampling board, 2.2 kW motor-generator, and 6RA70 controller, as illustrated in Fig. 8. A four-channel DA is introduced in DSP board to record and view all internal states, including the stator flux, electromagnetic torque, estimated and real speed, etc.

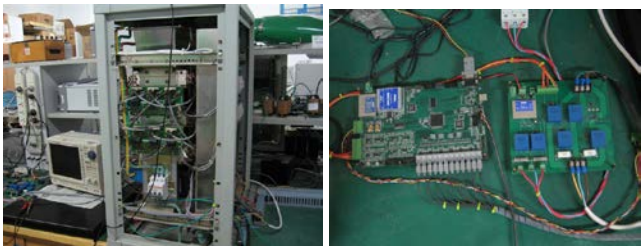

(a) 3-level inverter (b) DSP control board

(c) 2.2 kW motor-generator (d) 6RA70 controller

Figure 8. Experimental setup of the 3-level DTC drive

B. *Experimental Results*

Firstly the starting response without load is tested. In Fig. 9 the motor starts directly under step commanding value and the peak value reaches 16 A. As a comparison, the maximum starting current in Fig. 10 with pre-excitation does not exceed 10 A, which validates the effectiveness of the proposed pre-excitation technique.

Secondly the performance under external disturbance is tested and shown in Fig. 11. The full load is applied and removed suddenly when the motor is at steady operation of 1500 rpm. It is seen that the torque responses quickly while the stator flux is kept constant. However, there is some fall in speed. Analysis reveals the reason that the amplitude of synthesis vector is not large enough to provide enough output torque. This can be overcome by increasing the amplitude of synthesis vectors, or the value of DC bus. More flexible scheme can adjust the amplitude of synthesis vectors according to the range of speed and load condition. Despite this, it is seen that during the dynamic process, the estimated speed follows the real speed exactly, validating the effectiveness of the proposed observer.

Thirdly, four-quadrant operation is performed. Fig. 12 shows the operation between forward and reverse at 150 rpm. It is seen that the system exhibits excellent dynamic performance.

The line voltage at steady state of 1500 rpm shown in Fig. 13 proves that there is no high voltage jump and the switching is smooth, which validates the effectiveness of the proposed novel synthesis sequence in Section II.

Finally, the performance of low speed operation is presented. Fig. 14 and Fig. 15 show that the system can operate at very low speed of 6 rpm without load and 30 rpm with 80% the rated load, respectively. There are only slight oscillations in the speed, and the stator flux is smooth and steady.

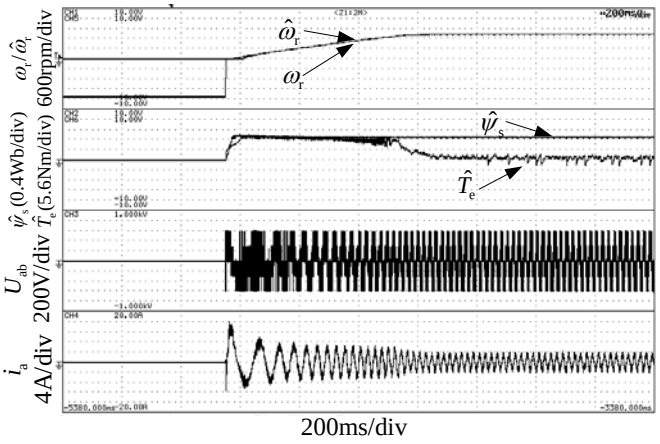

Figure 9. Starting up from 0 rpm to 1500 rpm without pre-excitation

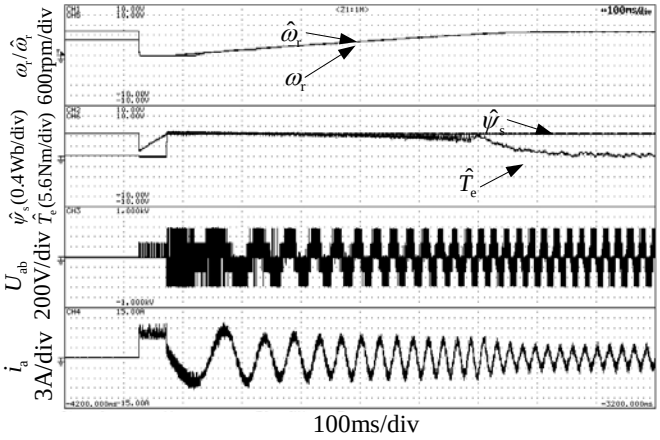

Figure 10. Staring up from 0 rpm to 1500 rpm with pre-excitation

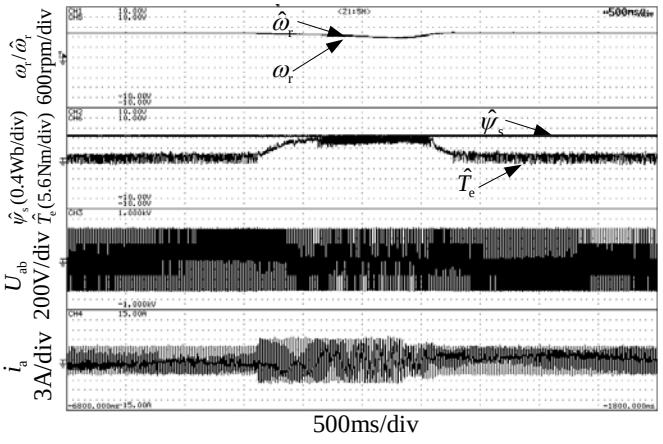

Figure 11. Response to external load disturbance

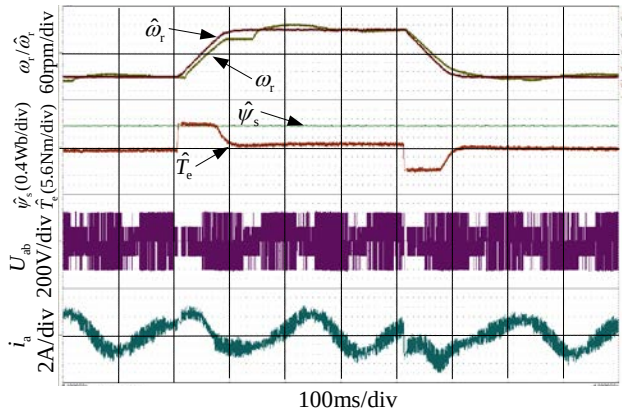

Figure 12. Four-quadrant operation

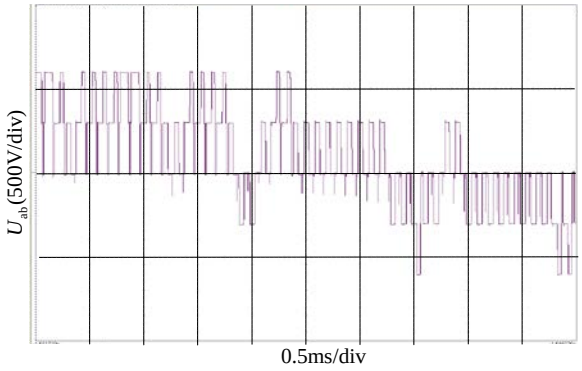

Figure 13. Zoomed line voltage at 1500 rpm

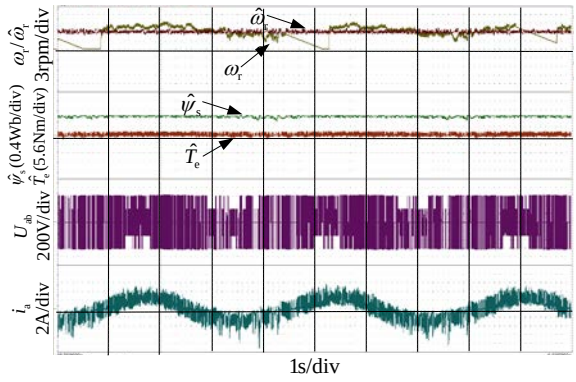

Figure 14. Low speed operation at 6 rpm without load

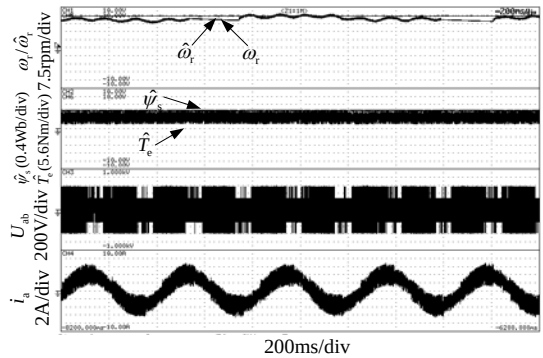

Figure 15. Low speed operation at 30 rpm with 80% the rated load

V. CONCLUSION

This paper proposes a sensorless 3-level inverter-fed DTC motor drive based on discrete space vector modulation. A novel vector synthesis sequence is proposed to solve the problems of neutral point unbalance and non-smooth vector switching caused by the topology of 3-level inverter. FLC and speed adaptive flux observer with load torque observation are incorporated in the system to enhance the low speed performance. Also, the issue of large starting current are investigated and solved by introducing the technique of pre-excitation. The presented experimental results exhibit excellent performance of the motor drive over a wide speed range.

REFERENCES

[1] I. Takahashi and T. Noguchi, "A new quick-response and high efficiency control strategy of an induction motor," *IEEE Trans. on Ind. Appl.*, vol. 22, no. 5, pp. 820-827,1986.

[2] M. Depenbrock, "Direct self control (DSC) of inverter-fed induction machine," *IEEE Trans. on Power Electron.*, vol. 3, no. 5, pp. 420-429, 1988.

[3] J. Rodriguez, J. S. Lai, and F. Z. Peng, "Multilevel inverters: a survey of topologies, controls, and applications," *IEEE Trans. Ind. Electron.*, vol. 49, no. 4, pp. 724-738 , 2002.

[4] G. S. Buja and M. P. Kazmierkowski. "Direct torque control of PWM inverter-fed AC motors - a survey," *IEEE Trans. on Ind. Electron.*, vol. 51, no. 4, pp. 744-757, 2004.

[5] T. G. Habetler, "Direct torque control of induction machines using space vector modulation," *IEEE Trans. Ind. Appl.*, vol. 28, no. 5, pp.1045-1053, 1992.

[6] D. Casadei, F. Profiuno, G. Serra, *et al.*, "FOC and DTC: two viable schemes for induction motors torque control," *IEEE Trans. Power Electron.*, vol. 17, no. 5, pp. 779-787, 2002.

[7] N. Celanovic and D. Boroyevich "A comprehensive study of neutral-point voltage balancing problem in three-level neutral-point-clamped voltage source PWM inverters," *IEEE Trans. Power Electron.*, vol. 15, no. 3, pp. 242–249, Mar. 2000.

[8] Yongchang Zhang and Zhengming Zhao, "Comparative study of PI, sliding mode and fuzzy logic controller for rotor field oriented controlled induction motor drives," in Proc. *IEEE Int. Conf. on Electrical Machines and Systems*, Wuhan, China, Oct. 2008.

[9] Yongchang Zhang, Zhengming Zhao, Ting Lu, *et al.*, "Sensorless 3-level inverter-fed induction motor drive based on indirect torque control," in Proc. *IEEE 6th Int. Power Electronics and Motion Control Conf.*, Wuhan, China, May 2009, pp. 589-593.